Mcc1229, an Stx2a-amplifying microcin, is produced *in vivo* and requires CirA for activity

Erin M. Nawrocki,[a] Laura E. Hutchins,[b] Kathryn A. Eaton,[b] Edward G. Dudley[a,c*]

[a]Department of Food Science, The Pennsylvania State University, University Park, PA, USA

[b]Department of Microbiology and Immunology, University of Michigan, Ann Arbor, MI, USA

[c]*E. coli* Reference Center, The Pennsylvania State University, University Park, PA, USA

Running Title: CirA is the Mcc1229 receptor

*Address correspondence to Edward G. Dudley, egd100@psu.edu

Abstract: 244 words

Body: 4810 words

Abstract

Enterohemorrhagic *E. coli* (EHEC) strains, including the foodborne pathogen *E. coli* O157:H7, are responsible for thousands of hospitalizations each year. Various environmental triggers can modulate pathogenicity in EHEC by inducing expression of Shiga toxin (Stx), which is encoded on a lambdoid prophage and transcribed together with phage late genes. Cell-free supernatants of the sequence type (ST) 73 *E. coli* strain 0.1229 are potent inducers of Stx2a production in EHEC, suggesting that 0.1229 secretes a factor that activates the SOS response and leads to phage lysis. We previously demonstrated that this factor, designated microcin (Mcc) 1229, was proteinaceous and plasmid-encoded. To further characterize Mcc1229 and support its classification as a microcin, we investigated its regulation, determined its receptor, and identified loci providing immunity. Production of Mcc1229 was increased upon iron limitation, as determined by ELISA, *lacZ* fusions, and qRT-PCR. Spontaneous Mcc1229-resistant mutants and targeted gene deletion revealed that CirA was the Mcc1229 receptor. TonB, which interacts with CirA in the periplasm, was also essential for Mcc1229 import. Subcloning of the Mcc1229 plasmid indicated that Mcc activity was neutralized by two ORFs, each predicted to encode a domain of unknown function (DUF)-containing protein. In a germfree mouse model of infection, colonization with 0.1229 suppressed subsequent colonization of EHEC. Although Mcc1229 was produced *in vivo*, it was dispensable for colonization suppression. The regulation, import, and immunity determinants identified here are consistent with features of other Mccs, suggesting that Mcc1229 be included in this class of small molecules.

Introduction

Enterohemorrhagic *Escherichia coli* (EHEC) are foodborne pathogens that can cause severe clinical complications, including hemorrhagic colitis (HC) and hemolytic uremic syndrome (HUS), through the production of Shiga toxin (Stx) and other virulence factors (1–3). Stx is encoded on a temperate lambdoid bacteriophage and is therefore induced via the bacterial SOS response (4–6). Certain antibiotics and DNA-damaging agents are known to trigger phage induction and increase the expression of Stx *in vivo* and *in vitro* (7, 8). In the intestinal environment, members of the microbiome and their metabolites can modulate the pathogenicity of EHEC strains in multiple ways (9). Commensal bacteria can reduce the growth and colonization of EHEC, broadly limiting virulence factor expression (10). Alternatively, strains that are sensitive to the *stx*-converting phage can be infected and thus amplify Stx production (11–13). Finally, small molecules such as bacteriocins that target EHEC can both inhibit growth and promote Stx expression by induction of the phage lytic cycle (14, 15).

Bacteriocin activity was first described nearly a century ago (16) and is widespread in *E. coli*, with up to 60% of strains identified as colicin producers in some surveys (17–19). Microcins, which have a lower molecular weight than colicins (20), are found less frequently and are not as well characterized (21). They are generally smaller than 10 kDa in size, are not SOS-induced, and are secreted by intact cells (22, 23). Foundational studies on microcin B17 (MccB17), MccJ25, and others revealed that microcins are typically expressed in stationary phase, when cells are starved for nutrients (24–26). In particular, iron-limiting conditions often stimulate microcin production (27–29). Some microcins are post-translationally modified with the addition of siderophores (30–32), and many colicins and microcins exploit siderophore receptors for entry into target cells (33, 34). Expression of bacteriocins in nutrient-poor environments can also confer a

fitness advantage to producing strains, allowing them to kill their competitors and better colonize a given niche (35–37). In mouse models, for example, iron limitation can be advantageous for either pathogens (38) or probiotic bacteria (39) that produce bacteriocins.

Prior studies of the human *E. coli* isolate 0.1229 revealed that cell-free supernatants from this strain were sufficient to induce the SOS response and increase the Stx expression of EHEC (15). Microcin B17, which is encoded on a 96.3 kb plasmid in 0.1229, contributed to but was not fully responsible for SOS induction or Stx amplification (15). An additional factor with Stx-amplifying activity was localized to p0.1229_3, a 12.9 kb plasmid in the strain (15). This activity was dependent on TolC for efflux from 0.1229 and TonB for import into the target cell (15). The SOS-inducing, Stx-amplifying agent of p0.1229_3 is presumed to be a new microcin, first described in strain 0.1229 and thus designated Mcc1229. Although the chemical identity of Mcc1229 is not known, it is encoded within a 5.2 kb region of p0.1229_3 whose annotations include hypothetical proteins, an ABC transporter, a cupin superfamily protein, and domain of unknown function (DUF)-containing proteins (15).

Only a small number of microcins have been purified, and their functions in complex environments like the gut microbiome are not well defined (21). Some have theorized that the microcins prevalent in phylogroup B2 *E. coli* enhance their ability to dominate the rectal niche and colonize the urinary tract (40). 0.1229 is a phylogroup B2 isolate of sequence type (ST) 73. Other members of ST73 are notable urinary pathogens (e.g. CFT073), and the lineage carries many virulence factors that can promote colonization and persistence *in vivo* (41, 42). In 0.1229, MccB17 and Mcc1229 may serve this purpose, as they are lethal to competing *E. coli* strains (15). To elucidate the role of the putative microcin Mcc1229, we have here clarified its export, import,

immunity, and regulation. We have also probed the effect of 0.1229 and its microcins in a germfree mouse model of EHEC infection.

Results

Stx2a levels are increased upon growth in supernatants of E. coli 0.1229 ΔB17::FRT

E. coli strain 0.1229 produces two microcins: microcin B17 and the lesser characterized Mcc1229 (15). To isolate the impact of Mcc1229, we deleted the microcin B17 operon by one-step recombination, generating 0.1229 ΔB17::FRT. Inactivation of both microcins was accomplished by one-step recombination of 0.1229 ΔB17::FRT with the Δ6::*cat* PCR product, which was previously designed to remove a hypothetical protein and an ABC transporter from the Mcc1229 cluster on p0.1229_3 (15). These ORFs were formerly described as Hp1 and ABC based on their predicted protein products (15). In accordance with microcin nomenclature and in reference to their role in amplifying Shiga toxin, we have assigned genes in the Mcc1229 region names that begin with *mctA* (microcin involved in toxin amplification). Hp1 and ABC have been renamed *mctA* and *mctB*, respectively, and therefore the Δ6::*cat* deletion will be now be referenced as Δ*mctAB*::*cat*.

To determine the effect of culture conditions and to optimize production of Mcc1229 for future studies, *E. coli* 0.1229 ΔB17::FRT was grown in various liquid media. These included LB with 0%, 0.5%, and 1% NaCl (no, low, and high salt, respectively) and M9 supplemented with casamino acids, thiamine, and 0.4% of glucose, glycerol, maltose, or fructose. Stx2a amplification by Mcc1229 was determined by culturing the stx_{2a}^{+} *E. coli* O157:H7 strain PA2 in spent supernatants. Supernatants from LB cultures of 0.1229 ΔB17::FRT amplified Stx2a to the greatest extent (Figure 1). Amplification was dependent on Mcc1229 production, as the supernatants of

0.1229 ΔB17::FRT Δ*mctAB*::*cat* (which produced neither MccB17 nor Mcc1229) were statistically equivalent to broth controls ($p = 0.9789$) and induced minimal levels of Stx2a (Figure 1).

Iron suppresses Stx2a-amplifying activity

To further investigate conditions influencing Mcc1229 expression, we added the metal chelating agents EDTA or 2,2'-bipyridyl (bipy) to cultures of 0.1229 ΔB17::FRT grown in LB with high salt. Supernatants from 0.1229 ΔB17::FRT cultures grown in LB + bipyridyl amplified Stx2a levels beyond those from LB alone (Figure 2). In the presence of low concentrations (10 μM) of ferric chloride, EDTA and bipyridyl supernatants still significantly amplified Stx2a above unsupplemented LB supernatant levels (Figure 2). When $FeCl_3$ levels were increased to 200 μM—equimolar to EDTA or bipyridyl—the Stx2a-amplifying effect of these supernatants was suppressed (Figure 2). In other words, excess iron negated the impact of bipyridyl on Mcc1229. By contrast, the addition of 200 μM $CaCl_2$, $MgCl_2$, or $MnCl_2$ to 0.1229 ΔB17::FRT cultures did not reduce their Stx2a-amplifying activity (data not shown), suggesting that this effect was specific to $FeCl_3$.

mctA, mctB, and mctC ORFs are required for Stx2a amplification

Prior work demonstrated that the p0.1229_3 plasmid, and specifically a 5.2 kb region therein, was sufficient to amplify Stx2a (15). This region was moved into the medium-copy pBR322 vector, replacing the *bla* gene (15). The resulting construct is termed pBR322::mcc1229. The mcc1229 region is predicted to encode three hypothetical proteins (MctA, MctF, and MctG), an ABC transporter (MctB), a cupin domain protein (MctC), and two domain of unknown function

proteins (MctD and MctE) (Figure 3a). Each of these was previously deleted by one-step recombination in the native 0.1229 strain, inserting a *cat* marker in its place on p0.1229_3. *mctA*, *mctB*, *mctC*, and *mctF* deletion mutants were significantly impaired for Stx2a amplification (15). To avoid any potential polar effects of the *cat* insertions, we here constructed markerless in-frame deletions of the same ORFs in the pBR322::mcc1229 clone instead. When the *mctA*, *mctB*, and *mctC* ORFs were deleted from this region, the resulting constructs no longer amplified Stx2a (Figure 3b). Supernatants from C600 (pBR322::mcc1229Δ*mctA*), C600 (pBR322::mcc1229Δ*mctB*), and C600 (pBR322::mcc1229Δ*mctC*) were indistinguishable from an empty vector control (Figure 3b). C600 (pBR322::mcc1229Δ*mctF*) and C600 (pBR322::mcc1229Δ*mctG*) were not diminished in their ability to amplify Stx2a (data not shown).

p0.1229_3 ORFs are in the Fur regulon

Sequence analysis of the Stx2a-amplifying region on p0.1229_3 revealed a putative Fur binding site [ataAATGATAActATTcTC, where uppercase letters indicate identity to the consensus (43)] upstream of the *mctA* open reading frame (Figure 3a). The region upstream of *mctA* was ligated into pRS551 and successfully promoted transcription of *lacZ* (Figure 4a). Promoter regions upstream of the *mctB*, *mctC*, and *mctE* ORFs were also verified in this manner (Figure 4a). Transcriptional activity of the *mctA* promoter decreased when supplemented with ferric chloride (Figure 4a), suggesting that MctA was regulated by iron. These data were supported by transcriptional analysis in 0.1229 and 0.1229 Δ*fur*::*cat*. qRT-PCR targeting *mctA*, *mctB*, *mctC*, and *mctE* regions indicated that expression of each gene was increased in the *fur* mutant (Figure 4b), consistent with a model in which the Fe-Fur complex repressed transcription of the microcin.

149 *CirA is the outer membrane receptor for Mcc1229*

150 To identify the receptor for Mcc1229, we investigated its entry into target cells in several
151 ways. First, in an agar overlay assay, we showed that Mcc1229 inhibited the susceptible *E. coli*
152 O157:H7 strain PA2, creating a zone of clearing around Mcc1229-producing colonies.
153 Spontaneous Mcc1229-resistant mutants of PA2 that grew within the zone of inhibition were then
154 subject to whole-genome sequencing. Three independent colonies revealed mutations that would
155 affect CirA expression: two contained frameshift mutations in the *cirA* ORF that introduce a
156 premature stop codon, and one carried an 86 bp deletion directly upstream of the *cirA* start codon
157 (Table 1). These isolates (PA2.1, PA2.2, and PA2.3) were insensitive to Stx2a amplification by
158 0.1229 ΔB17::*cat* supernatants (Figure 5). Second, a targeted deletion of *cirA* in PA2 by one-step
159 recombination (Δ*cirA*::*kan*) was also resistant to Mcc1229-mediated Stx2a amplification (Figure
160 5). Sensitivity was restored by complementation with the medium-copy number pBR322::*cirA*
161 (Figure 5). Finally, *cirA* was confirmed as the Mcc1229 receptor using a set of indicator strains
162 bearing mutations in known colicin receptors (44). While a wild-type indicator strain was
163 susceptible to Mcc1229 inhibition in the agar overlay method, a *cirA* mutant was resistant to this
164 microcin (data not shown).
165
166 *Mcc1229 entry requires TonB*
167 CirA is a known TonB-dependent transporter, and the import of CirA-dependent colicins
168 requires the activity of TonB in the periplasm (45). Earlier data also implicated TonB in SOS
169 induction by Mcc1229 in a reporter strain (15). We next sought to inactivate *tonB* in *E. coli*
170 O157:H7 to determine its role in Stx2a amplification by Mcc1229. Attempts to delete *tonB* in the
171 PA2 background by various methods were unsuccessful. *tonB* was instead deleted by one-step

recombination in EDL933, a well-characterized $stx_{1a}^{+}stx_{2a}^{+}$ O157:H7 strain (46). A Δ*tonB*::*cat* mutant did not amplify Stx2a in response to supernatants containing Mcc1229 (Figure 6). When complemented with a plasmid copy of *tonB* (pKP315), the strain behaved as wildtype (Figure 6). These data indicated that CirA and TonB were both necessary for Stx2a amplification by Mcc1229.

Immunity to Mcc1229 is mediated by the mctD-mctE region of p0.1229_3

The lethality of colicins and microcins necessitates a mechanism of protection for the producing cell. By cloning progressively smaller fragments of p0.1229_3 into pBR322, we identified a region of the plasmid that was sufficient to confer immunity to Mcc1229. Two adjacent ORFs, *mctD* and *mctE*, each predicted to encode a domain of unknown function (DUF)-containing protein, protected MG1655 from Mcc1229-mediated killing (Figure 7a). Vectors containing either of the single ORFs were not protective (Figure 7a). When the pBR322::*mctDE* construct was transformed into PA2, PA2 became insensitive to 0.1229 ΔB17::*cat* supernatant and Stx2a production did not increase (Figure 7b).

Mcc1229 is expressed in vivo but is not required for suppression of PA2

To determine the effect of microcins *in vivo*, we colonized germfree mice with *E. coli* 0.1229 and its derivatives and collected fecal samples at one day post infection. After suspending feces in LB, samples were centrifuged to pellet the solid matter and the supernatant spotted atop a suspension of the PA2 test strain. Supernatants from mice infected with 0.1229 inhibited the growth of PA2, but those from mice infected with a Mcc1229 knockout strain had no effect (Figure 8a and 8b).

The role of Mcc1229 in the germfree mouse model of EHEC was investigated by sequential inoculation of 0.1229 and PA2. Mice were first infected with 0.1229 or its derivatives, then with PA2 seven days later. Monoinfections of 0.1229 or PA2 served as controls. PA2 alone was able to colonize at concentrations of between $10^8 – 10^{10}$ CFU/g and caused symptoms consistent with Stx-mediated disease including colitis and acute kidney injury (47, 48). When mice were colonized with 0.1229 prior to the introduction of PA2, PA2 colonization was almost fully suppressed. PA2 was recovered from the cecal contents of only six of 65 mice coinfected with 0.1229 or its derivatives (Figure 8c, Table 2). This effect did not require Mcc1229 or MccB17, however, as the single and double microcin mutants of 0.1229 were capable of suppressing PA2 equivalent to the wildtype (Figure 8c, Table 2). Colonization suppression was not protective against disease, as PA2 was still lethal to coinfected mice and Stx was detected in feces from all groups (Figure 8d, Table 3). This likely indicates that PA2 was present at some time during infection but was either lost or suppressed below the limit of detection.

Discussion

A putative microcin from the human *E. coli* isolate 0.1229 was previously shown to induce the SOS response and Stx expression in target strains (15). Here, we have confirmed the activity of this microcin (Mcc1229), isolated its activity from that of a second microcin encoded by 0.1229 (MccB17), and further characterized its production, regulation, and effects. Like several other colicins and microcins, Mcc1229 uses the CirA siderophore receptor (Figure 5) and the TonB complex (Figure 6) for entry into a target cell. CirA was first identified as the colicin I receptor and is also used by colicin/microcin V (33, 49). In the producing strain, evidence suggests that Mcc1229 requires the *mctABC* region of plasmid p0.1229_3 for activity (Figure 3b). Open reading

frames similar to *mctA*, with cysteine-rich C-terminal regions and cognate ABC transporters, are also consistent with typical microcin operons (50).

The functional contributions of the cupin-like *mctC* and DUF-containing *mctD-mctE* ORFs in the Mcc1229 cluster have not yet been elucidated. In our system, the *mctDE* region conferred immunity to Mcc1229 killing and Stx amplification (Figure 7), but it is not clear whether the DUF-containing proteins encoded by *mctD* and *mctE* directly interact with the microcin. Current Pfam records indicate that the DUF2164 domain present in MctE is found in 804 protein sequences in 715 species, but it is not associated with a clan or superfamily (51). DUF4440, which is found in MctD, belongs to a family in the nuclear transport factor (NTF) 2 clan, which includes numerous proteins with enzymatic and non-enzymatic functions (52). Some proteins with NTF2-like folds are known to provide immunity to bacterial toxins, but their sequences (Pfam PF15655) are diverse and dissimilar to the DUF4440 domain in MctD (53). Proteins with DUF4440 and/or NTF2-like domains have also been shown to operate in polyketide biosynthesis pathways, where they are involved in catalyzing the formation of natural products (54, 55). Some proteins with cupin domains have enzymatic activity (56, 57), so it is possible that the p0.1229_3 MctC is involved in processing or modification of Mcc1229. Because our attempts to complement the *mctA*, *mctB*, and *mctC* deletion mutants *in trans* were unsuccessful (data not shown), we cannot speculate further on the contributions of these ORFs to Mcc1229 production.

Beyond its cellular export and import, the observed Fe-Fur regulation of Mcc1229 further supports its classification as a microcin. Mcc1229's amplification of Stx was increased in the presence of chelating agents, and this effect could be reversed by the addition of iron specifically (Figure 2). Moreover, the expression of *mctA*, *mctB*, *mctC,* and *mctE* genes were increased in a Δ*fur*::*cat* background (Figure 4b). Taken together, these data likely indicate that Mcc1229 is

transcriptionally repressed by the canonical Fe-Fur complex (58). A similar pattern is seen in the regulation of microcin E492 in *Klebsiella pneumoniae* (29). Like the site upstream of *mceX* in the MccE492 operon, the putative Fur box upstream of *mctA* is 68% (13/19 nt) identical to the consensus Fur sequence described for *E. coli* (59, 60). Fur-regulated microcins may provide a competitive advantage for *E. coli* strains *in vivo*, where iron availability is restricted (61, 62). The Fur regulon is essential for survival of various *E. coli* pathotypes *in vivo* (63–65), and the B2 phylogroup of *E. coli* (which includes 0.1229) is associated with a high prevalence of microcin genes (66).

In our study, microcin Mcc1229 was produced *in vivo* but had no effect on EHEC colonization or disease (Figure 8). Nevertheless, we observed a striking example of suppression by *E. coli* 0.1229 in which PA2 was rarely if ever recovered from coinfections. Most other *E. coli* do not suppress EHEC to the same extent, although there is precedent for colonization suppression by the probiotic strain Nissle 1917 (67, 68). Intriguingly, Nissle and 0.1229 both belong to ST73, a lineage frequently isolated from ExPEC infections (69). ST73 strains carry a broad assortment of virulence factors, including many genes for adherence and iron acquisition that could provide a selective advantage over competitors (70). Ongoing studies may determine whether colonization resistance is a trait that is common to ST73.

Interactions with the microbiome can alter the virulence of EHEC in numerous ways. Understanding these effects will help predict the unique pathogenicity and disease outcomes of a given infection. Here, we have expanded upon the attributes of Mcc1229, a new *E. coli* microcin that induces the SOS response and amplifies Stx2a expression *in vitro*. When characterizing the interplay of Mcc1229 and EHEC *in vivo*, however, we found that microcin activity was not a significant contributor to EHEC virulence or to colonization efficiency. This discrepancy

highlights the need for additional research regarding the dynamics of bacteriocin expression in the intestinal environment. The regulation, stability, and activity spectrum of bacteriocins all influence their physiological role, as do external factors such as inflammation and nutrient availability. Although Mcc1229 could be unified with other microcins based on the cellular factors described in this work, its actual ecological impact was not apparent from our germfree mouse model and awaits further clarification.

Materials and Methods

Bacterial strains and culture conditions

E. coli strains were routinely grown in lysogeny broth (LB; 10 g/l tryptone, 5 g/l yeast extract, 10 g/l NaCl) at 37°C and maintained in 20% glycerol at -80°C. Minimal medium (M9) was formulated with 12.8 g/l $Na_2HPO_4 \cdot 7H_2O$, 3 g/l KH_2PO_4, 0.5 g/l NaCl, 1 g/l NH_4Cl, 2 mM $MgSO_4$, and 0.1 mM $CaCl_2$. M9 was supplemented with 0.1% casamino acids, 0.005% thiamine, and 0.4% of the desired carbon source. Mueller-Hinton (MH) agar was prepared according to the manufacturer's instructions. EDTA, 2,2'-bipyridyl, $FeCl_3$, $CaCl_2$, $MgCl_2$, and $MnCl_2$ were added to media at 0.2 mM. Antibiotics were used as follows: ampicillin, 50 µg/ml; chloramphenicol, 12.5 µg/ml; kanamycin, 25 µg/ml; tetracycline, 10 µg/ml. All media components were purchased from BD Difco (Franklin Lakes, NJ) and all enzymes from New England Biolabs (NEB; Ipswich, MA) unless otherwise noted.

One-step recombination

E. coli knockouts were constructed according to the protocol of Datsenko and Wanner (71). Primers incorporating 40 bp immediately upstream and downstream of the gene of interest were used to amplify the *cat* cassette from pKD3 or the *kan* cassette from pKD4 (Table 1). The target strain was first transformed with pKD46 and grown to mid-log phase, then induced with 0.02 M L-arabinose for 1 h. Cells were washed with cold water and 10% glycerol and electroporated with the *cat* or *kan* PCR product using a GenePulser II instrument (2.5 kV, 0.2 cm gap cuvettes; Bio-Rad, Hercules, CA). Transformants were verified by colony PCR with primers approximately 200 bp up- and downstream of the gene of interest, and the site of the insertion was confirmed by Sanger sequencing (Table 1). Mutants were complemented with a plasmid copy of the gene of

interest, cloned into the medium-copy number vector pBR322 by Gibson assembly (72). Assembly primers were designed using NEBuilder (https://nebuilder.neb.com; Table 1). Amplicons were purified with the QIAquick Cleanup Kit (Qiagen, Germantown, MD) and assembled with the Gibson Assembly Cloning Kit according to the manufacturers' instructions. Assembly junctions were likewise confirmed with colony PCR and Sanger sequencing (Table 1).

Because multiple efforts to inactivate *tonB* in PA2 by one-step recombination were unsuccessful, we generated a Δ*tonB*::*cat* mutant in the EDL933 background. This mutant was complemented by pKP315, kindly provided by Dr. Kathleen Postle, which carries an arabinose-inducible copy of *tonB*. L-arabinose was added to EDL933 cultures at 0.3%.

LacZ fusions

Transcriptional activity was measured by fusing selected p0.1229_3 fragments to a promoterless *lacZ* gene in the pRS551 vector (73). Fragments were amplified from p0.1229_3 using the given primers (Table 1) and digested with EcoRI-HF and BamHI-HF enzymes. The products were cleaned up using the QIAquick kit and ligated into an EcoRI-BamHI digest of pRS551. Ligation mixtures were transformed into chemically competent DH5α cells (New England Biolabs) and verified by miniprep and restriction digests. Constructs were then electroporated into *E. coli* 0.1229. Reporter strains were cultured in LB, shaking at 37˚C, and grown until mid-logarithmic phase. Cells were then harvested and suspended in Z buffer. LacZ activity was measured by the hydrolysis of *o*-nitrophenyl-β-D-galactoside according to the method of Miller *et al.* (74).

qPCR

RNA was extracted from 16 h LB cultures of 0.1229 and 0.1229 Δ*fur*::*cat* using TRIzol (ThermoFisher Scientific, Waltham, MA). Genomic DNA was removed by digestion with RQ1 RNase-Free DNase (Promega, Madison, WI) and RNA converted to cDNA using the ThermoScript RT-PCR system (ThermoFisher). Expression of *mctA*, *mctB*, *mctC*, and *mctE* genes was quantified in 20 µl reactions using PerfeCTa SYBR Green FastMix (Quantabio, Beverly, MA) and 200 nM qPCR primers (Table 1) on a QuantStudio3 instrument (ThermoFisher). To validate the efficiency (>95%) of each primer pair, its target was amplified from genomic DNA and purified in a spin column cleanup kit (Dot Scientific Inc., Burton, MI). The concentration of this product was measured by spectrophotometry (NanoDrop 1000, ThermoFisher) and ten-fold dilutions ranging from 10^{-2} through 10^{-7} ng/µl were used as templates in qPCR. A standard curve was constructed from the resulting Ct values. Differences in gene expression between wildtype and Δ*fur*::*cat* strains were determined by the ΔΔCt method, using the 16S ribosomal RNA *rrsH* gene as an internal control (75).

In-frame deletions and site-directed mutagenesis

Prior work demonstrated that a fragment of the p0.1229_3 plasmid encompassing nucleotides 2850 through 7950 was sufficient to amplify Stx when cloned into pBR322 (15). In-frame deletions of individual ORFs in this vector, pBR322::mcc1229, were generated with NEB's Q5 Site-Directed Mutagenesis Kit. Primers facing outward from the chosen ORF were designed with the NEBaseChanger tool and used with Q5 polymerase to amplify a linear fragment from pBR322::mcc1229 (Table 1). This product was treated with KLD enzyme cocktail to digest template DNA and recircularize the plasmid according to the manufacturer's instructions. Constructs were confirmed by PCR of DH5α transformant colonies using VF/VR primers (Table

338 1). Mutations were then verified by Sanger sequencing and plasmids electroporated into C600 as
339 described above to assure that no wildtype copies remained.
340
341 *Inhibition assays*
342 Microcin production was evaluated by measuring inhibition of a target strain in agar
343 overlays (76). The microcin-producing strain was spot-inoculated on MH agar and incubated at
344 37°C for approximately 24 h. Plates were inverted over filter paper discs impregnated with 300 µl
345 chloroform for 30 minutes to kill producing cells. Cultures of the target strains were then
346 suspended to 0.05 OD_{600} per ml in soft (0.7%) nutrient agar, poured atop the plates, and allowed
347 to solidify. After overnight incubation at 37°C, inhibition was noted by the presence of halos
348 surrounding a microcin-producing colony. Zones of inhibition were quantified by subtracting the
349 diameter of the producing colony from the diameter of the clear zone surrounding it. Spontaneous
350 mutants growing within the zones of inhibition were restreaked to purify and retested in agar
351 overlays to confirm microcin resistance. Known microcin and colicin producers and their
352 corresponding indicator strains were from the NCTC reference set, kindly provided by Dr. Robert
353 F. Roberts (44).
354 For inhibition assays using supernatants, plates were inoculated with the test strain in soft
355 agar as described above. Fecal samples from mice colonized with 0.1229 or its derivatives were
356 collected at 1 day after inoculation with PA2, suspended in 100-200 µL LB broth, and centrifuged.
357 Ten µl of supernatant were spotted atop the test strain and allowed to dry before overnight
358 incubation at 37°C.
359
360 *Whole-genome sequencing and bioinformatics*

Genomic DNA was extracted from overnight cultures using the DNeasy Blood and Tissue Kit (Qiagen). Libraries were prepared using the Nextera XT kit (Illumina, San Diego, CA) and sequenced on the MiSeq platform, generating 2×250 bp reads. Reads were assembled in the Galaxy workspace with the SPAdes tool (77), and single nucleotide polymorphisms were identified using Snippy (78), comparing to the reference genome assembly GCA_000335355.2. Putative Fur binding sites and promoter motifs were identified by analysis of the p0.1229_3 sequence with RSAT (79) and BPROM (80), respectively.

Coculture and supernatant experiments

Supernatants of *E. coli* 0.1229 and its derivatives were harvested after 16 h shaking at 37°C and passed through 0.2 µm cellulose acetate filters (VWR Life Sciences, Radnor, PA). Assays to quantify Stx amplification were performed as previously described (15). Briefly, the test strain of *E. coli* was suspended in 1 ml of spent supernatant to 0.05 OD_{600} and inoculated atop solid LB agar in a 6-well plate (BD Biosciences Inc., Franklin Lakes, NJ).

For Stx assays, the test strains were *E. coli* O157:H7 isolates. PA2 (81) was used routinely as it demonstrated the greatest Stx amplification in prior experiments (13). EDL933 (46) was used in the event that a PA2 mutant could not be obtained. Strains were diluted to 0.05 OD_{600} in either broth or filtered supernatant and inoculated atop solid LB agar in 6-well plates. Cultures were then incubated statically at 37°C for 8 h. Aliquots of each culture were removed to measure OD_{620}, and the remaining volume was treated with 6 mg/ml polymyxin B for 5 min at 37°C to release intracellular Stx. Samples were then centrifuged for 5 min to pellet cell debris and supernatants were collected and stored at -80°C until use in an R-ELISA.

384 *R-ELISA*

385 Shiga toxin was detected in a receptor-based ELISA as previously described (14). A
386 microtiter plate was first coated with 25 µg/ml ceramide trihexosides (Matreya Biosciences,
387 Pleasant Gap, PA) in methanol. The methanol was evaporated and the plate subsequently blocked
388 with 4% bovine serum albumin in phosphate buffered saline containing 0.05% Tween 20 (PBST).
389 Supernatant samples were diluted in PBS as necessary and added to wells for 1 h, gently shaking
390 at room temperature. Monoclonal anti-Stx2 antibody was purchased from Santa Cruz Biotech
391 (Santa Cruz, CA) and added to wells at 1 µg/ml for 1 h. Anti-mouse secondary antibody conjugated
392 to horseradish peroxidase was purchased from MilliporeSigma (Burlington, MA) and also added
393 at 1 µg/ml for 1 h. Between each of the preceding steps, the plate was washed five times with
394 PBST. One-step Ultra TMB (ThermoFisher) was then used for detection. The plate was incubated
395 for approximately 5 min before the reaction was stopped with the addition of 2 M H_2SO_4 and the
396 A_{450} was measured (Multiskan FC, ThermoFisher). A standard curve was established using serial
397 dilutions of lysate from PA11, a high Stx2a-producer (81). The concentration of Stx2a in *E. coli*
398 O157:H7 samples was determined by comparison to this curve and is reported in µg/ml,
399 normalized to the OD_{620} of each *E. coli* O157:H7 culture.
400
401 *Animal experiments*
402 Male and female Swiss-Webster mice aged 3 to 5 weeks were raised in the University of
403 Michigan germfree colony. They were housed in soft-sided bubble isolators or sterile isocages and
404 fed autoclaved water and laboratory chow *ad libitum*. Throughout the experiment, the mice
405 received sterile food, water, and bedding to maintain germfree conditions, except for the infecting

406 *E. coli* strains. All animal experiments were conducted with the approval of the University of
407 Michigan Animal Care and Use Committee.

408 Mice were infected orally with ~10^6 CFU of each *E. coli* inoculum. In coinfection
409 experiments, 0.1229 and its derivatives were inoculated first and were followed by PA2 one week
410 later. Mice were weighed prior to each inoculation and just prior to euthanasia. They were
411 evaluated daily for evidence of illness (dehydration, ruffled coat, or reluctance to move) and were
412 euthanized 1 or 7 days after PA2 infection or when they became moribund. Prior to euthanasia,
413 evidence of illness was recorded, and at necropsy, samples were collected for bacterial culture,
414 Stx2 ELISA, and histologic examination.

415 For bacterial culture, samples of the cecal contents were weighed, serially diluted in sterile
416 LB broth, and cultured on sorbitol-MacConkey (SMaC) agar. PA2 is non-sorbitol-fermenting and
417 appears as white colonies on SMaC plates. Cultures from co-colonized mice were quantified based
418 on the number of pink or white colonies. For quantification of Stx2, the cecal contents were stored
419 at −20°C until evaluation with a Premier EHEC ELISA kit (Meridian Biosciences Inc., Cincinnati,
420 OH). The concentration of Stx2a was determined by comparison to the PA11 standard curve
421 discussed above (81).

References

1. Griffin PM, Tauxe R V. 1991. The epidemiology of infections caused by *Escherichia coli* O157:H7, other enterohemorrhagic *E. coli*, and the associated hemolytic uremic syndrome. Epidemiol Rev 13:60–98.
2. Nguyen Y, Sperandio V, Padola NL, Starai VJ. 2012. Enterohemorrhagic *E. coli* (EHEC) pathogenesis. Front Cell Infect Microbiol 2:1–7.
3. Croxen MA, Law RJ, Scholz R, Keeney KM, Wlodarska M, Finlay BB. 2013. Recent advances in understanding enteric pathogenic *Escherichia coli*. Clin Microbiol Rev 26:822–880.
4. Scotland SM, Smith HR, Willshaw GA, Rowe B. 1983. Vero cytotoxin production in strain of *Escherichia coli* is determined by genes carried on bacteriophage. Lancet 322:216.
5. Ptashne M. 2004. A genetic switch: phage lambda revisited. Cold Spring Harbor Laboratory Press, Cold Spring Harbor, NY.
6. Wagner PL, Neely MN, Zhang X, Acheson DW, Waldor MK, Friedman DI. 2001. Role for a phage promoter in Shiga toxin 2 expression from a pathogenic *Escherichia coli* strain. J Bacteriol 183:2081–2085.
7. Zhang X, McDaniel AD, Wolf LE, Keusch GT, Waldor MK, Acheson DWK. 2000. Quinolone antibiotics induce Shiga toxin–encoding bacteriophages, toxin production, and death in mice. J Infect Dis 181:664–670.
8. Toshima H, Yoshimura A, Arikawa K, Hidaka A, Ogasawara J, Hase A, Masaki H, Nishikawa Y. 2007. Enhancement of Shiga toxin production in enterohemorrhagic *Escherichia coli* serotype O157:H7 by DNase colicins. Appl Environ Microbiol 73:7582–

7588.

9. Nawrocki EM, Mosso HM, Dudley EG. 2020. A toxic environment: a growing understanding of how microbial communities affect *Escherichia coli* O157:H7 Shiga toxin expression. Appl Environ Microbiol 86.

10. de Sablet T, Chassard C, Bernalier-Donadille A, Vareille M, Gobert AP, Martin C. 2009. Human microbiota-secreted factors inhibit Shiga toxin synthesis by enterohemorrhagic *Escherichia coli* O157:H7. Infect Immun 77:783–790.

11. Gamage SD, Strasser JE, Chalk CL, Weiss AA. 2003. Nonpathogenic *Escherichia coli* can contribute to the production of Shiga toxin. Infect Immun 71:3107–3115.

12. Gamage SD, Patton AK, Strasser JE, Chalk CL, Weiss AA. 2006. Commensal bacteria influence *Escherichia coli* O157:H7 persistence and Shiga toxin production in the mouse intestine. Infect Immun 74:1977–83.

13. Goswami K, Chen C, Xiaoli L, Eaton KA, Dudley EG. 2015. Coculture of *Escherichia coli* O157:H7 with a nonpathogenic *E. coli* strain increases toxin production and virulence in a germfree mouse model. Infect Immun 83:4185–4193.

14. Xiaoli L, Figler HM, Goswami K, Dudley EG. 2018. Nonpathogenic *E. coli* enhance Stx2a production of *E. coli* O157:H7 through *bamA*-dependent and independent mechanisms. Front Microbiol 9:1–13.

15. Mosso HM, Xiaoli L, Banerjee K, Hoffmann M, Yao K, Dudley EG. 2020. A putative microcin amplifies Shiga toxin 2a production of *Escherichia coli* O157:H7. J Bacteriol 202.

16. Reeves P. 1965. The bacteriocins. Bacteriol Rev 29:24–45.

17. Gordon DM, Riley MA, Pinou T. 1998. Temporal changes in the frequency of

colicinogeny in *Escherichia coli* from house mice. Microbiology 144:2233–2240.

18. Riley MA, Gordon DM. 1992. A survey of Col plasmids in natural isolates of *Escherichia coli* and an investigation into the stability of Col-plasmid lineages. J Gen Microbiol 138:1345–1352.

19. Feldgarden M, Riley MA. 1998. High levels of colicin resistance in *Escherichia coli*. Evolution (N Y) 52:1270–1276.

20. Asensio C, Pérez-Díaz JC, Martínez MC, Baquero F. 1976. A new family of low molecular weight antibiotics from enterobacteria. Biochem Biophys Res Commun 69.

21. Baquero F, Lanza VF, Baquero M-R, Del Campo R, Bravo-Vázquez DA. 2019. Microcins in *Enterobacteriaceae*: peptide antimicrobials in the eco-active intestinal chemosphere. Front Microbiol 10:2261.

22. Duquesne S, Destoumieux-Garzón D, Peduzzi J, Rebuffat S. 2007. Microcins, gene-encoded antibacterial peptides from enterobacteria. Nat Prod Rep 24:708.

23. Baquero F, Moreno F. 1984. The microcins. FEMS Microbiol Lett 23:117–124.

24. Connell N, Han Z, Moreno F, Kolter R. 1987. An *E. coli* promoter induced by the cessation of growth. Mol Microbiol 1:195–201.

25. Chiuchiolo MJ, Delgado MA, Farías RN, Salomón RA. 2001. Growth-phase-dependent expression of the cyclopeptide antibiotic microcin J25. J Bacteriol 183:1755–1764.

26. Moreno F, Gónzalez-Pastor JE, Baquero M-R, Bravo D. 2002. The regulation of microcin B, C and J operons. Biochimie 84:521–529.

27. Salomón R. 1994. Influence of iron on microcin 25 production. FEMS Microbiol Lett 121:275–280.

28. Poey ME, Azpiroz MF, Laviña M. 2006. Comparative analysis of chromosome-encoded

491 microcins. Antimicrob Agents Chemother 50:1411–1418.
492 29. Marcoleta AE, Gutiérrez-Cortez S, Hurtado F, Argandoña Y, Corsini G, Monasterio O,
493 Lagos R. 2018. The ferric uptake regulator (Fur) and iron availability control the
494 production and maturation of the antibacterial peptide microcin E492. PLoS One
495 13:e0200835.
496 30. Nolan EM, Fischbach MA, Koglin A, Walsh CT. 2007. Biosynthetic tailoring of microcin
497 E492m: post-translational modification affords an antibacterial siderophore-peptide
498 conjugate. J Am Chem Soc 129:14336–14347.
499 31. Vassiliadis G, Peduzzi J, Zirah S, Thomas X, Rebuffat S, Destoumieux-Garzon D. 2007.
500 Insight into siderophore-carrying peptide biosynthesis: enterobactin is a precursor for
501 microcin E492 posttranslational modification. Antimicrob Agents Chemother 51:3546–
502 3553.
503 32. Vassiliadis G, Destoumieux-Garzon D, Lombard C, Rebuffat S, Peduzzi J. 2010. Isolation
504 and characterization of two members of the siderophore-microcin family, microcins M
505 and H47. Antimicrob Agents Chemother 54:288–297.
506 33. Chehade H, Braun V. 1988. Iron-regulated synthesis and uptake of colicin V. FEMS
507 Microbiol Lett 52:177–181.
508 34. Braun V, Patzer SI, Hantke K. 2002. Ton-dependent colicins and microcins: modular
509 design and evolution. Biochimie 84:365–380.
510 35. Gillor O, Giladi I, Riley MA. 2009. Persistence of colicinogenic *Escherichia coli* in the
511 mouse gastrointestinal tract. BMC Microbiol 9:1–7.
512 36. Majeed H, Gillor O, Kerr B, Riley MA. 2011. Competitive interactions in *Escherichia coli*
513 populations: the role of bacteriocins. ISME J 5:71–81.

514 37. Riley MA. 2011. Bacteriocin-Mediated Competitive Interactions of Bacterial Populations
515 and Communities, p. 13–26. *In* Prokaryotic Antimicrobial Peptides. Springer New York,
516 New York, NY.
517 38. Nedialkova LP, Denzler R, Koeppel MB, Diehl M, Ring D, Wille T, Gerlach RG, Stecher
518 B. 2014. Inflammation fuels colicin Ib-dependent competition of *Salmonella* serovar
519 Typhimurium and *E. coli* in enterobacterial blooms. PLoS Pathog 10:e1003844.
520 39. Sassone-Corsi M, Nuccio S, Liu H, Hernandez D, Vu CT, Takahashi AA, Edwards RA,
521 Raffatellu M. 2016. Microcins mediate competition among *Enterobacteriaceae* in the
522 inflamed gut. Nature 540:280–283.
523 40. Massip C, Oswald E. 2020. Siderophore-microcins in *Escherichia coli*: determinants of
524 digestive colonization, the first step toward virulence. Front Cell Infect Microbiol.
525 41. Vejborg RM, Friis C, Hancock V, Schembri MA, Klemm P. 2010. A virulent parent with
526 probiotic progeny: comparative genomics of *Escherichia coli* strains CFT073, Nissle 1917
527 and ABU 83972. Mol Genet Genomics 283:469–484.
528 42. Salvador E, Wagenlehner F, Köhler C-D, Mellmann A, Hacker J, Svanborg C, Dobrindt
529 U. 2012. Comparison of asymptomatic bacteriuria *Escherichia coli* isolates from healthy
530 individuals versus those from hospital patients shows that long-term bladder colonization
531 selects for attenuated virulence phenotypes. Infect Immun 80:668–678.
532 43. Stojiljkovic I, Bäumler AJ, Hantke K. 1994. Fur regulon in Gram-negative bacteria:
533 Identification and characterization of new iron-regulated *Escherichia coli* genes by a Fur
534 titration assay. J Mol Biol 236:531–545.
535 44. Murinda SE, Roberts RF, Wilson RA. 1996. Evaluation of colicins for inhibitory activity
536 against diarrheagenic *Escherichia coli* strains, including serotype O157:H7. Appl Environ

Microbiol 62:3196–3202.

45. Curtis NAC, Eisenstadt RL, East SJ, Cornford RJ, Walker LA, White AJ. 1988. Iron-regulated outer membrane proteins of *Escherichia coli* K-12 and mechanism of action of catechol-substituted cephalosporins. Antimicrob Agents Chemother 32:1879–1886.

46. Perna NT, Plunkett G, Burland V, Mau B, Glasner JD, Rose DJ, Mayhew GF, Evans PS, Gregor J, Kirkpatrick HA, Pósfai G, Hackett J, Klink S, Boutin A, Shao Y, Miller L, Grotbeck EJ, Davis NW, Lim A, Dimalanta ET, Potamousis KD, Apodaca J, Anantharaman TS, Lin J, Yen G, Schwartz DC, Welch RA, Blattner FR. 2001. Genome sequence of enterohaemorrhagic *Escherichia coli* O157:H7. Nature 409:529–533.

47. Eaton KA, Friedman DI, Francis GJ, Tyler JS, Young VB, Haeger J, Abu-Ali G, Whittam TS. 2008. Pathogenesis of renal disease due to enterohemorrhagic *Escherichia coli* in germ-free mice. Infect Immun 76:3054–3063.

48. Eaton KA, Fontaine C, Friedman DI, Conti N, Alteri CJ. 2017. Pathogenesis of colitis in germ-free mice infected with EHEC O157:H7. Vet Pathol 54:710–719.

49. Cardelli J, Konisky S. 1974. Isolation and characterization of an *Escherichia coli* mutant tolerant to colicins Ia and Ib. J Bacteriol 119:379–385.

50. Vassiliadis G, Destoumieux-Garzón D, Peduzzi J. 2011. Class II Microcins, p. 309–332. *In* Drider, D, Rebuffat, S (eds.), Prokaryotic Antimicrobial Peptides: From Genes to Applications. Springer New York, New York, NY.

51. Mistry J, Chuguransky S, Williams L, Qureshi M, Salazar GA, Sonnhammer ELL, Tosatto SCE, Paladin L, Raj S, Richardson LJ, Finn RD, Bateman A. 2021. Pfam: The protein families database in 2021. Nucleic Acids Res 49.

52. Eberhardt RY, Chang Y, Bateman A, Murzin AG, Axelrod HL, Hwang WC, Aravind L.

2013. Filling out the structural map of the NTF2-like superfamily. BMC Bioinformatics 14.

53. Zhang D, de Souza RF, Anantharaman V, Iyer LM, Aravind L. 2012. Polymorphic toxin systems: Comprehensive characterization of trafficking modes, processing, mechanisms of action, immunity and ecology using comparative genomics. Biol Direct 7.

54. Huang T, Chang CY, Lohman JR, Rudolf JD, Kim Y, Chang C, Yang D, Ma M, Yan X, Crnovcic I, Bigelow L, Clancy S, Bingman CA, Yennamalli RM, Babnigg G, Joachimiak A, Phillips GN, Shen B. 2016. Crystal structure of SgcJ, an NTF2-like superfamily protein involved in biosynthesis of the nine-membered enediyne antitumor antibiotic C-1027. J Antibiot (Tokyo) 69.

55. Vuksanovic N, Zhu X, Serrano DA, Siitonen V, Metsa-Ketel M, Melan CE, Silvaggi NR. 2020. Structural characterization of three noncanonical NTF2-like superfamily proteins: Implications for polyketide biosynthesis. Acta Crystallogr Sect F Struct Biol Commun 76.

56. Dunwell JM. 1998. Cupins: a new superfamily of functionally diverse proteins that Include germins and plant storage proteins. Biotechnol Genet Eng Rev 15:1–32.

57. Dunwell JM, Purvis A, Khuri S. 2004. Cupins: the most functionally diverse protein superfamily? Phytochemistry 65:7–17.

58. Troxell B, Hassan HM. 2013. Transcriptional regulation by ferric uptake regulator (Fur) in pathogenic bacteria. Front Cell Infect Microbiol 3.

59. Lundrigan MD, Kadner RJ. 1986. Nucleotide sequence of the gene for the ferrienterochelin receptor FepA in *Escherichia coli*. Homology among outer membrane receptors that interact with TonB. J Biol Chem 261:10797–10801.

60. Escolar L, Pérez-Martín J, De Lorenzo V. 1998. Binding of the Fur (ferric uptake

583 regulator) repressor of *Escherichia coli* to arrays of the GATAAT sequence. J Mol Biol.
584 61. Martin P, Tronnet S, Garcie C, Oswald E. 2017. Interplay between siderophores and
585 colibactin genotoxin in *Escherichia coli*. IUBMB Life 69:435–441.
586 62. Ganz T. 2009. Iron in innate immunity: starve the invaders. Curr Opin Immunol.
587 63. Zhu C, Ngeleka M, Potter AA, Allan BJ. 2002. Effect of *fur* mutation on acid-tolerance
588 response and in vivo virulence of avian septicemic *Escherichia coli*. Can J Microbiol
589 48:458–462.
590 64. Huja S, Oren Y, Biran D, Meyer S, Dobrindt U, Bernhard J, Becher D, Hecker M, Sorek
591 R, Ron EZ. 2014. Fur is the master regulator of the extraintestinal pathogenic *Escherichia*
592 *coli* response to serum. MBio 5.
593 65. Porcheron G, Dozois CM. 2015. Interplay between iron homeostasis and virulence: Fur
594 and RyhB as major regulators of bacterial pathogenicity. Vet Microbiol.
595 66. Micenková L, Bosák J, Štaudová B, Kohoutová D, Čejková D, Woznicová V, Vrba M,
596 Ševčíková A, Bureš J, Šmajs D. 2016. Microcin determinants are associated with B2
597 phylogroup of human fecal *Escherichia coli* isolates. Microbiologyopen 5:490–498.
598 67. Leatham MP, Banerjee S, Autieri SM, Mercado-Lubo R, Conway T, Cohen PS. 2009.
599 Precolonized human commensal *Escherichia coli* strains serve as a barrier to *E. coli*
600 O157:H7 growth in the streptomycin-treated mouse intestine. Infect Immun 77:2876–
601 2886.
602 68. Maltby R, Leatham-Jensen MP, Gibson T, Cohen PS, Conway T. 2013. Nutritional basis
603 for colonization resistance by human commensal *Escherichia coli* strains HS and Nissle
604 1917 against *E. coli* O157:H7 in the mouse intestine. PLoS One 8:e53957.
605 69. Manges AR, Geum HM, Guo A, Edens TJ, Fibke CD, Pitout JDD. 2019. Global

606 extraintestinal pathogenic *Escherichia coli* (ExPEC) lineages. Clin Microbiol Rev 32.
607 70. Bogema DR, McKinnon J, Liu M, Hitchick N, Miller N, Venturini C, Iredell J, Darling
608 AE, Roy Chowdury P, Djordjevic SP. 2020. Whole-genome analysis of extraintestinal
609 *Escherichia coli* sequence type 73 from a single hospital over a 2 year period identified
610 different circulating clonal groups. Microb Genomics 6.
611 71. Datsenko KA, Wanner BL. 2000. One-step inactivation of chromosomal genes in
612 *Escherichia coli* K-12 using PCR products. Proc Natl Acad Sci 97:6640–6645.
613 72. Gibson DG, Young L, Chuang R-Y, Venter JC, Hutchison CA, Smith HO. 2009.
614 Enzymatic assembly of DNA molecules up to several hundred kilobases. Nat Methods
615 6:343–345.
616 73. Simons RW, Houman F, Kleckner N. 1987. Improved single and multicopy *lac*-based
617 cloning vectors for protein and operon fusions. Gene 53:85–96.
618 74. Miller JH. 1972. Experiments in molecular genetics, pp. 352-355. Cold Spring Harb Lab
619 Press Cold Spring Harb Lab NY.
620 75. Abu-Ali GS, Ouellette LM, Henderson ST, Whittam TS, Manning SD. 2010. Differences
621 in adherence and virulence gene expression between two outbreak strains of
622 enterohaemorrhagic *Escherichia coli* O157:H7. Microbiology 156.
623 76. Pugsley AP, Oudega B. 1987. Methods of studying colicins and their plasmids, p. 105–
624 161. *In* Hardy, KG (ed.), Plasmids, a Practical Approach. IRL Press.
625 77. Bankevich A, Nurk S, Antipov D, Gurevich AA, Dvorkin M, Kulikov AS, Lesin VM,
626 Nikolenko SI, Pham S, Prjibelski AD, Pyshkin AV, Sirotkin AV, Vyahhi N, Tesler G,
627 Alekseyev MA, Pevzner PA. 2012. SPAdes: a new genome assembly algorithm and its
628 applications to single-cell sequencing. J Comput Biol 19:455–477.

78. Seemann T. 2015. Snippy: Rapid haploid variant calling and core SNP phylogeny. GitHub.

79. Nguyen NTT, Contreras-Moreira B, Castro-Mondragon JA, Santana-Garcia W, Ossio R, Robles-Espinoza CD, Bahin M, Collombet S, Vincens P, Thieffry D, van Helden J, Medina-Rivera A, Thomas-Chollier M. 2018. RSAT 2018: regulatory sequence analysis tools 20th anniversary. Nucleic Acids Res 46:W209–W214.

80. Solovyev V, Salamov A. 2011. Automatic annotation of microbial genomes and metagenomic sequences, p. 62–78. *In* Metagenomics and its Applications in Agriculture, Biomedicine and Environmental Studies.

81. Hartzell A, Chen C, Lewis C, Liu K, Reynolds S, Dudley EG. 2011. *Escherichia coli* O157:H7 of genotype lineage-specific polymorphism assay 211111 and clade 8 are common clinical isolates within Pennsylvania. Foodborne Pathog Dis 8:763–768.

82. Tatusova T, DiCuccio M, Badretdin A, Chetvernin V, Nawrocki EP, Zaslavsky L, Lomsadze A, Pruitt KD, Borodovsky M, Ostell J. 2016. NCBI prokaryotic genome annotation pipeline. Nucleic Acids Res 44:6614–6624.

83. Turatsinze J-V, Thomas-Chollier M, Defrance M, van Helden J. 2008. Using RSAT to scan genome sequences for transcription factor binding sites and cis-regulatory modules. Nat Protoc 3:1578–1588.

84. Livak KJ, Schmittgen TD. 2001. Analysis of relative gene expression data using real-time quantitative PCR and the 2-ΔΔCT method. Methods 25:402–408.

85. Appleyard RK. 1954. Segregation of new lysogenic types during growth of a doubly lysogenic strain derived from *Escherichia coli* K12. Genetics 39:440–52.

86. Blattner FR, Plunkett G, Bloch CA, Perna NT, Burland V, Riley M, Collado-Vides J,

652 Glasner JD, Rode CK, Mayhew GF, Gregor J, Davis NW, Kirkpatrick HA, Goeden MA,
653 Rose DJ, Mau B, Shao Y. 1997. The complete genome sequence of *Escherichia coli* K-12.
654 Science (80-) 277:1453–62.
655 87. Riley LW, Remis RS, Helgerson SD, McGee HB, Wells JG, Davis BR, Hebert RJ, Olcott
656 ES, Johnson LM, Hargrett NT, Blake PA, Cohen ML. 1983. Hemorrhagic colitis
657 associated with a rare *Escherichia coli* serotype. N Engl J Med 308:681–685.
658 88. Cherepanov PP, Wackernagel W. 1995. Gene disruption in *Escherichia coli*: TcR and
659 KmR cassettes with the option of Flp-catalyzed excision of the antibiotic-resistance
660 determinant. Gene 158:9–14.
661 89. Guzman LM, Belin D, Carson MJ, Beckwith J. 1995. Tight regulation, modulation, and
662 high-level expression by vectors containing the arabinose PBAD promoter. J Bacteriol
663 177:4121–4130.
664 90. Larsen RA, Thomas MG, Postle K. 1999. Protonmotive force, ExbB and ligand-bound
665 FepA drive conformational changes in TonB. Mol Microbiol 31:1809–1824.
666 91. Bolivar F, Rodriguez RL, Greene PJ, Betlach MC, Heyneker HL, Boyer HW, Crosa JH,
667 Falkow S. 1977. Construction and characterization of new cloning vehicle. II. A
668 multipurpose cloning system. Gene 2:95–113.
669

Figures

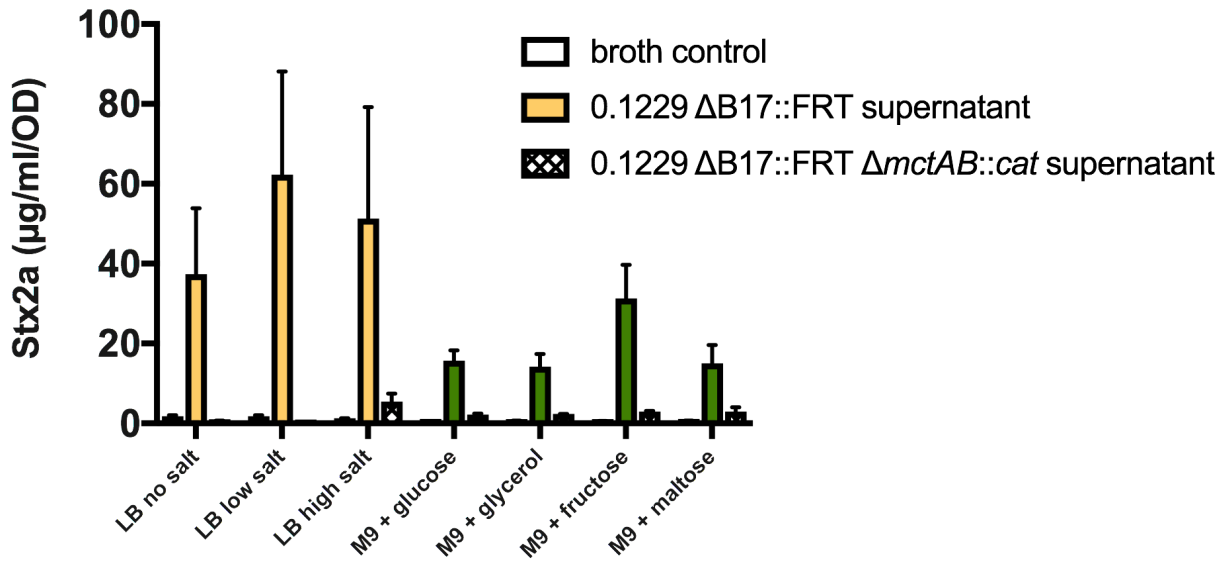

Figure 1. Stx2a levels are amplified by culture supernatants from rich media. Cell-free supernatants of *E. coli* 0.1229 ΔB17::FRT grown in various media were used to culture the *E. coli* O157:H7 strain PA2. Stx2a levels were measured by R-ELISA and normalized to the OD_{620} of each culture; the mean + SEM are reported (minimum n = 3). M9 medium was supplemented with 0.1% casamino acids, 0.005% thiamine, and 0.4% of the given carbon source. Cultures grown in spent supernatants of 0.1229 ΔB17::FRT are indicated by filled bars (yellow for LB, green for M9). Cultures grown in spent supernatants of the double microcin mutant, 0.1229 ΔB17::FRT Δ*mctAB*::*cat*, are given as crosshatched bars. For comparison, PA2 was grown in fresh media of the same composition, as indicated by empty bars. All such "broth control" cultures yielded less than 5 µg/ml/OD Stx2a.

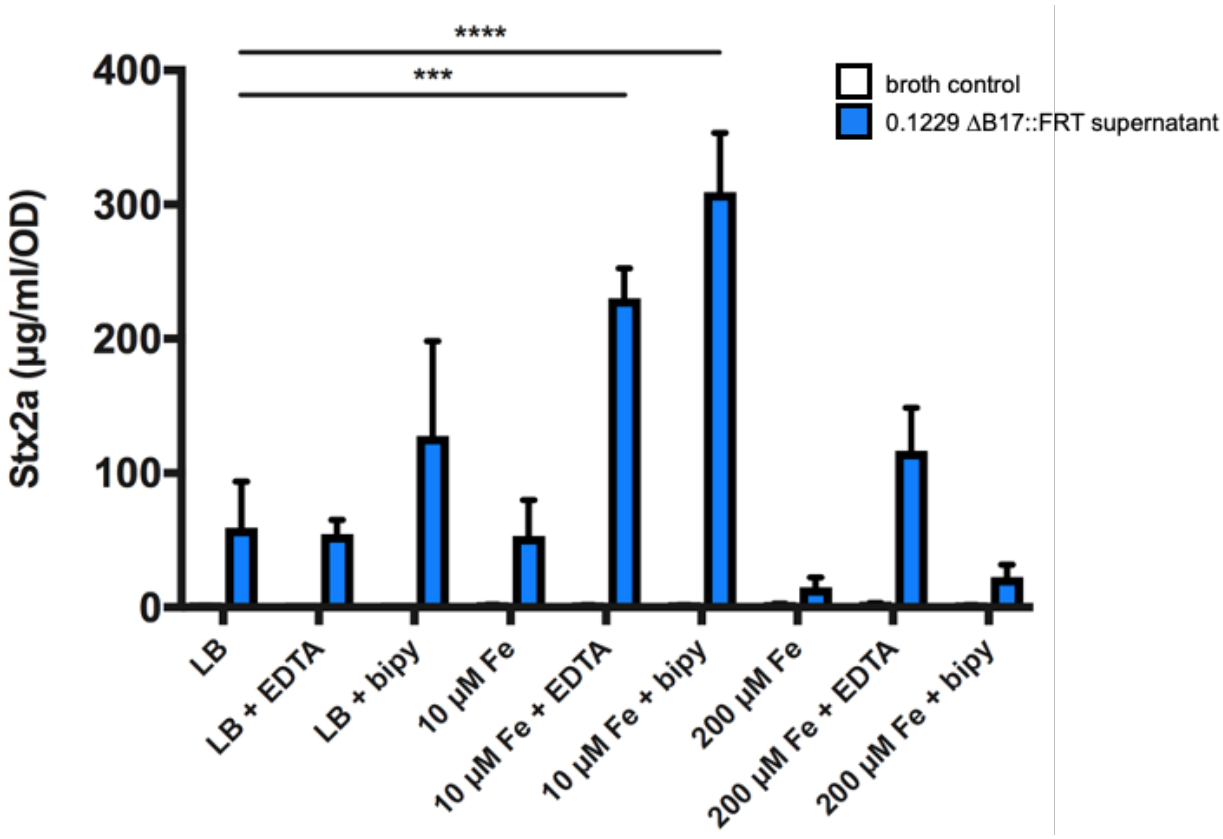

Figure 2. Stx2a levels are diminished when grown in supernatants from high-iron media. Cell-free supernatants of *E. coli* 0.1229 ΔB17::FRT grown in various media were used to culture the *E. coli* O157:H7 strain PA2. For comparison, PA2 was grown in fresh media of the same composition, as indicated by "broth control." Stx2a levels were measured by R-ELISA and normalized to the optical density of each culture; the mean + SEM are reported (n = 3 in all except 10 µM Fe cultures, for which n = 2). The metal chelators EDTA and 2,2'-bipyridyl (bipy) were added to media at 0.2 mM. Statistical significance was determined by two-way ANOVA and Sidek's multiple comparisons test, assigning LB as the standard for the broth control and 0.1229 ΔB17::FRT supernatant groups (***, $p < 0.001$; ****, $p < 0.0001$).

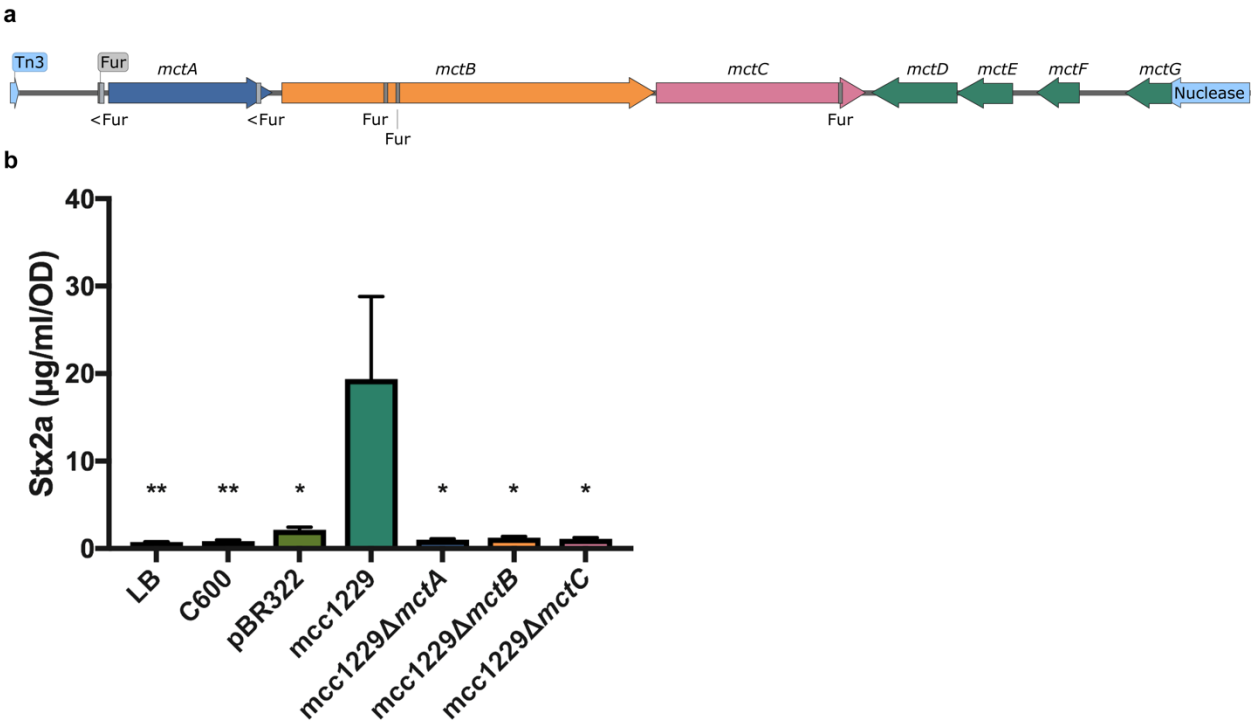

Figure 3. A 5.2 kb region of p0.1229_3 sufficient for Stx2a amplification encodes seven putative open reading frames and six predicted Fur binding sites. (a) Annotation of p0.1229_3 was performed by NCBI's Prokaryotic Genomes Automatic Annotation Pipeline (PGAAP) as reported previously (15, 82). Fur sites were identified by the matrix-scan algorithm at the RSAT Prokaryotes webserver (79, 83). Those on the reverse strand are indicated by <. The map diagram was generated by SnapGene software (from GSL Biotech; available at snapgene.com). (b) The mcc1229 region of p0.1229_3 was cloned into pBR322 and was sufficient to amplify Stx2a. Supernatants from the C600 strain alone or from the empty vector pBR322 did not amplify Stx2a. Stx2a expression of PA2 exposed to filtered culture supernatants was determined by ELISA as previously described. Values that differed significantly from the mcc1229 supernatant are marked with asterisks (*, $p < 0.05$; **, $p < 0.01$). Statistical analysis was performed by one-way ANOVA with Dunnett's multiple comparisons test.

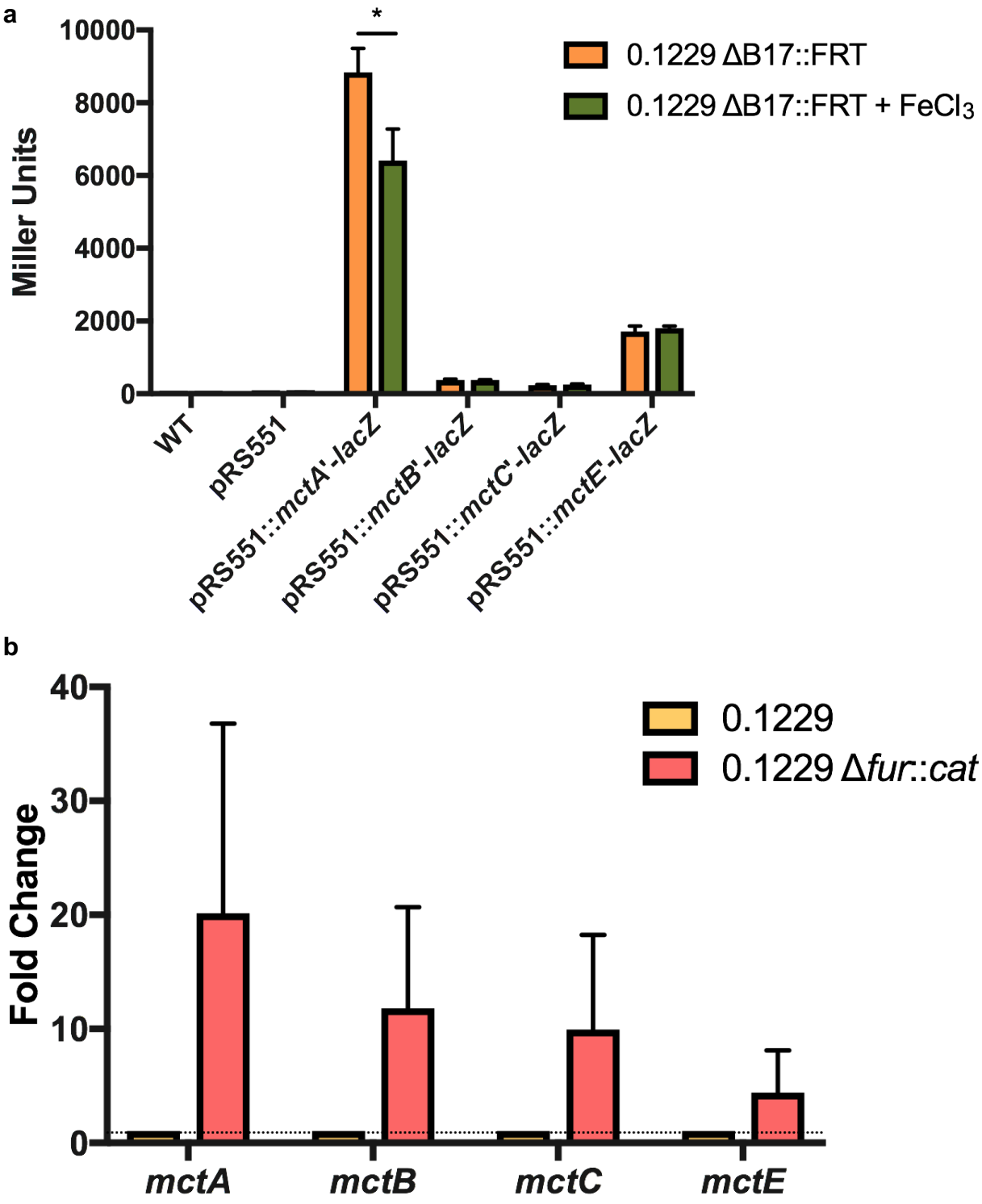

Figure 4. Mcc1229 transcription is iron-regulated. (a) A region upstream of the *mctA* ORF containing a putative Fur binding site was ligated into pRS551 and successfully promoted transcription of *lacZ*. Promoter regions upstream of the *mctB*, *mctC*, and *mctE* ORFs were also

tested in this manner. Transcriptional activity of the *mctA* promoter decreased when the medium was supplemented with 200 µM $FeCl_3$. Significance was determined by two-way ANOVA with Sidak's multiple comparisons test. (b) RNA was extracted from 16 h LB cultures of 0.1229 and 0.1229 Δ*fur*::*cat*, converted to cDNA, and probed by qPCR for the *mctA*, *mctB*, *mctC*, and *mctE* ORFs. Gene expression relative to wildtype was determined by the $\Delta\Delta C_T$ method using the ribosomal gene *rrsH* as an internal control (84). All Mcc1229 genes were consistently upregulated in the Δ*fur*::*cat* strain but the difference was not statistically significant by two-way ANOVA.

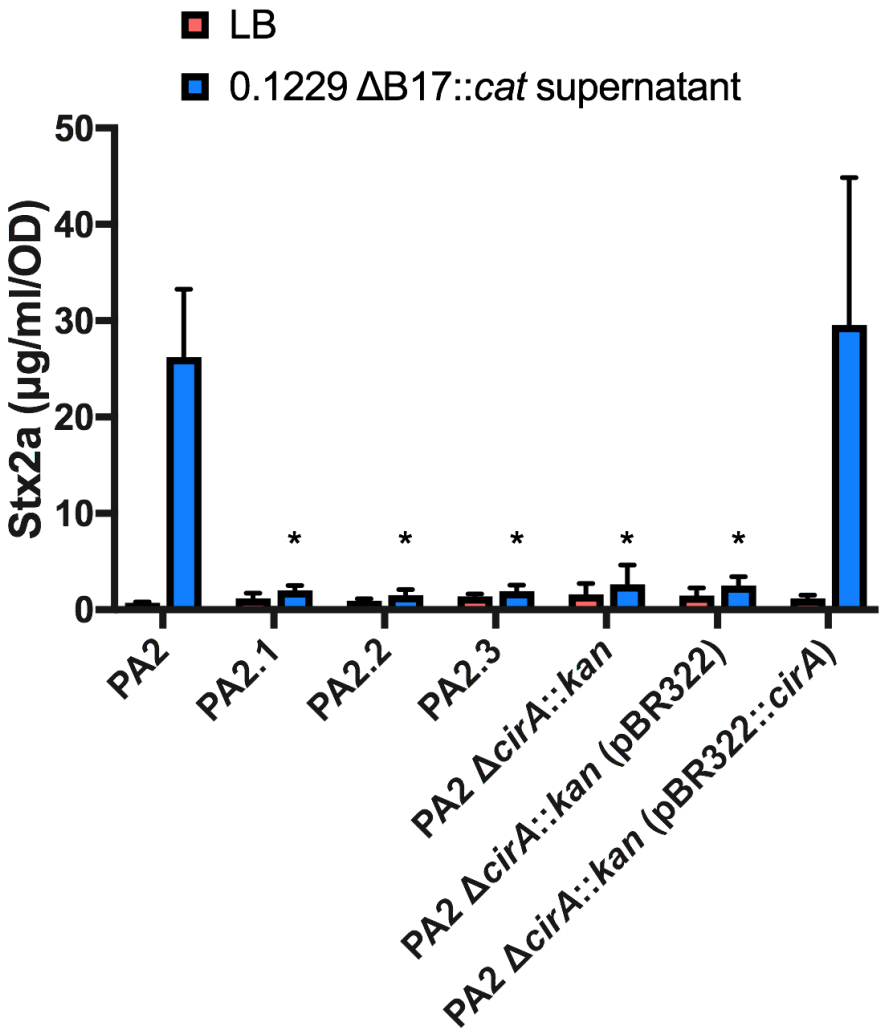

Figure 5. CirA is the outer membrane receptor for Mcc1229. Spontaneous mutants of PA2 were resistant to inhibition by *E. coli* 0.1229 Δ*B17*::*cat*. Colonies were isolated from within the zones of clearing and subject to whole genome sequencing to identify the source of Mcc1229 resistance. Multiple independent mutants (PA2.1, PA2.2, PA2.3) had mutations in CirA. A Δ*cirA*::*kan* mutant of PA2 is resistant to Mcc1229, and when *cirA* mutants are grown in spent supernatants of *E. coli* 0.1229 Δ*B17*::*cat*, they are insensitive to Stx amplification. Sensitivity is restored by complementation with pBR322::*cirA*. Asterisks mark significant difference between a given supernatant sample and the PA2 wildtype (two-way ANOVA, Dunnett's multiple comparisons test).

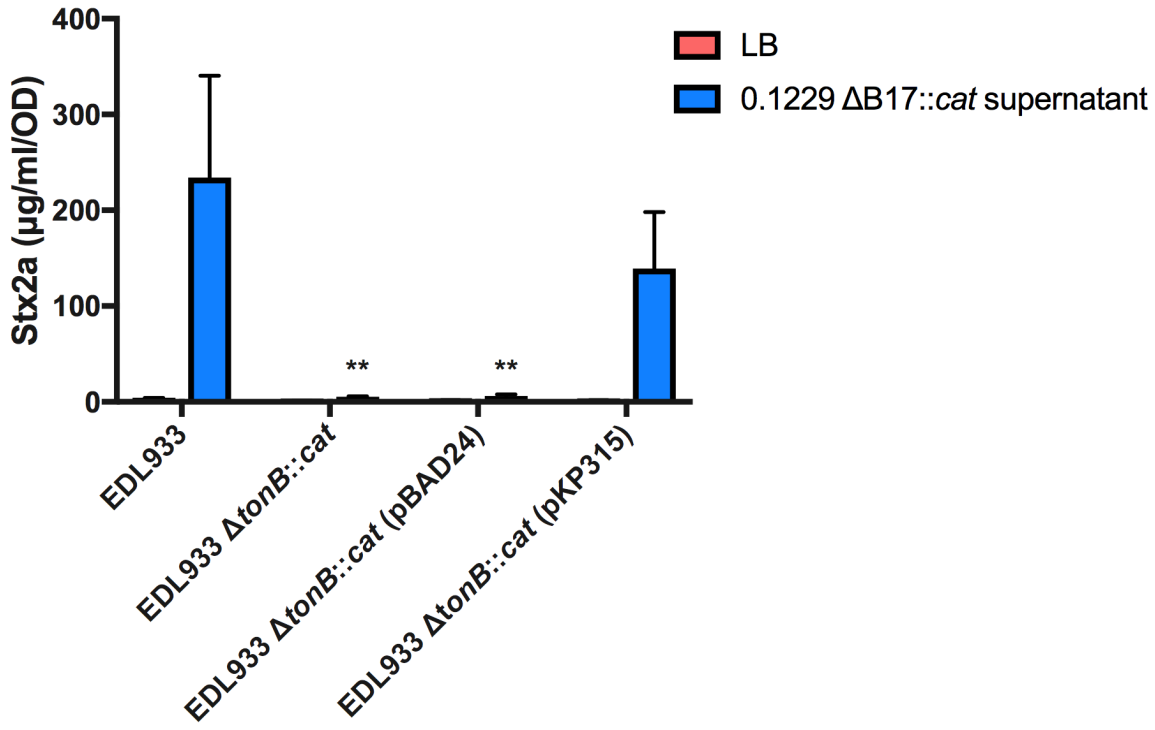

Figure 6. TonB is required for Mcc1229 activity. The periplasmic energy transducing protein TonB was deleted from *E. coli* O157:H7 strain EDL933 by one-step recombination. The resulting mutant does not increase Stx expression in response to spent supernatants containing Mcc1229. Activity is restored upon complementation with a plasmid copy of *tonB*, carried on pKP315. Because *tonB* is under P_{araC} control on pKP315, all strains in this experiment were grown in the presence of arabinose. Asterisks mark significant difference between a given supernatant sample and the EDL933 wildtype (two-way ANOVA, Dunnett's multiple comparisons test).

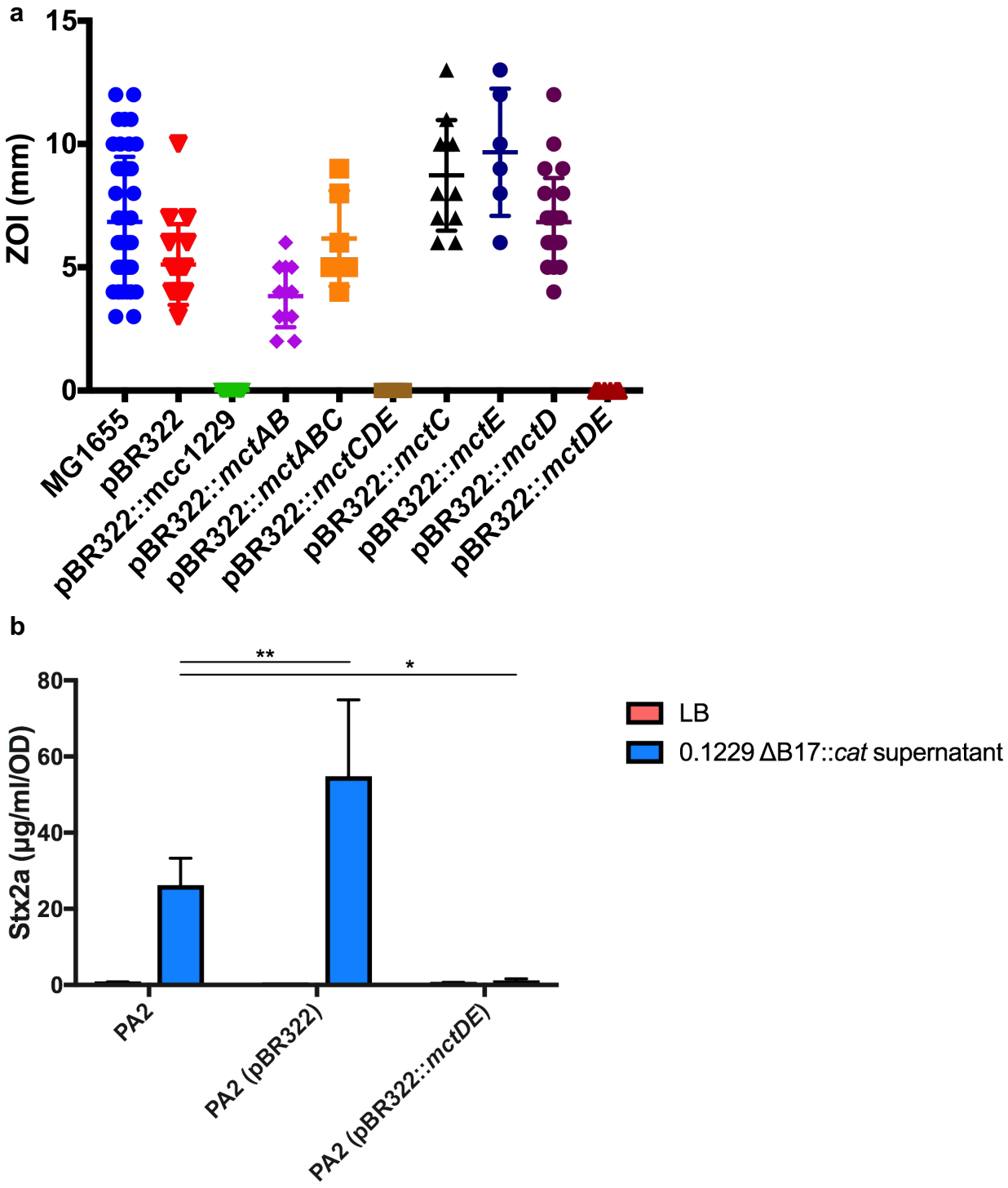

Figure 7. The *mctD-mctE* region is sufficient to confer immunity to Mcc1229. (a) Two p0.1229_3 ORFs annotated as proteins with domains of unknown function were cloned into pBR322 and transformed into *E. coli* strain MG1655. MG1655 carrying an empty vector is

740 sensitive to Mcc1229 produced by *E. coli* 0.1229 Δ*B17*::*cat*. MG1655 carrying pBR322::*mctDE*
741 is fully resistant to the microcin. (b) Transformants of PA2 carrying pBR322::*mctDE* do not
742 increase Stx expression when grown in spent supernatants of *E. coli* 0.1229 Δ*B17*::*cat*. Asterisks
743 mark significant difference between a given supernatant sample and the PA2 wildtype (two-way
744 ANOVA, Dunnett's multiple comparisons test; *, $p < 0.05$; **, $p < 0.01$).

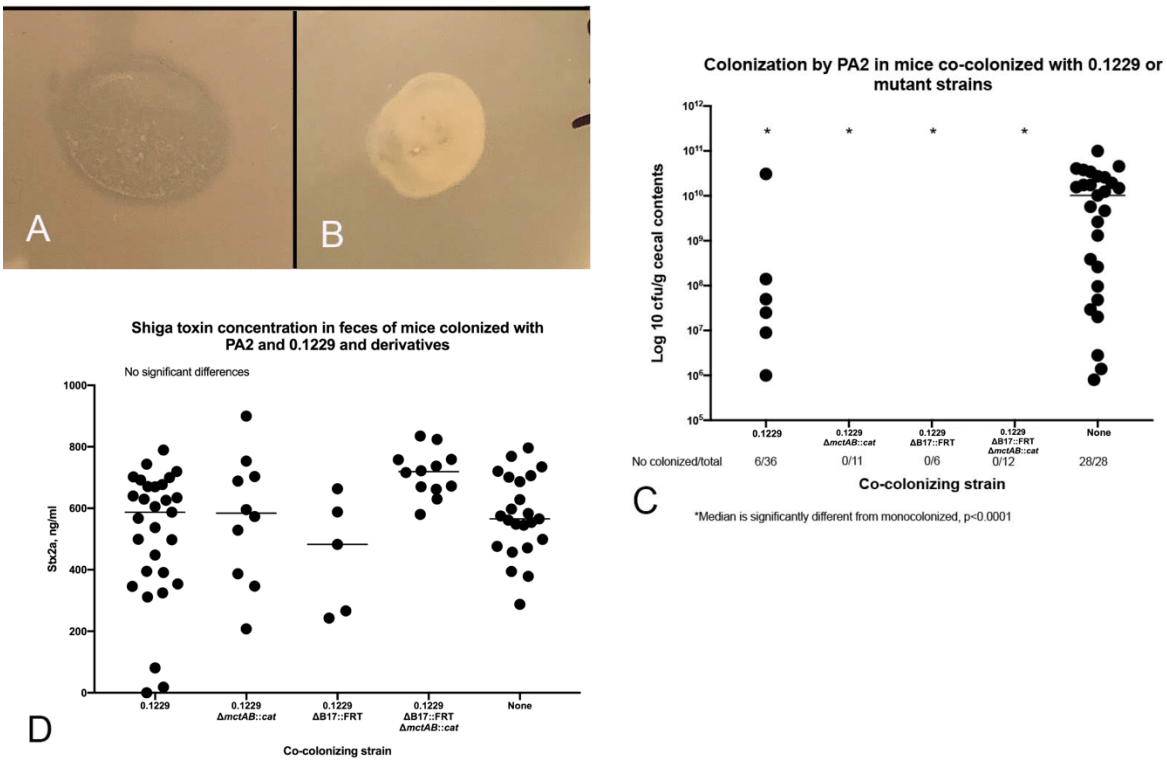

Figure 8. (a) and (b) Soft agar containing a suspension of PA2 was overlaid on LB, allowed to solidify, and fecal supernatants from infected mice were spotted on the overlay. Plates were incubated overnight at 37˚C. (a) Fecal supernatants from mice co-colonized with 0.1229 and PA2 prevented growth of PA2, resulting in a zone of clearing in the soft agar. (b) Supernatants from mice colonized with 0.1229 ΔB17::FRT Δ*mctAB*::*cat* did not affect PA2 growth. (c) PA2 colonization in co-colonized mice. PA2 colonization was detectable in only 16% of mice co-colonized by wild-type 0.1229 and in none of the mice colonized by 0.1229 Δ*mctAB*::*cat*, 0.1229 ΔB17::FRT, or 0.1229 ΔB17::FRT Δ*mctAB*::*cat.* In contrast 100% of mice inoculated with PA2 alone became colonized (also see Table 2). (d) Low colonization level did not affect Stx production. Stx was detected in all mouse groups and concentration ranged from 18 to 900 ng/ml. There were no differences between groups.

Tables

Table 1. Strains, primers, and plasmids.

Strain	*Characteristics*	*Reference*
C600	K-12 derivative	(85)
MG1655	K-12 derivative	(86)
0.1229	O18:H1, B2 phylogroup, AmpR, TetR	(15)
0.1229 ΔB17::*cat*	p0.1229_2Δ*mcbABCDEFG*::*cat*, AmpR, TetR, CamR	(15)
0.1229 ΔB17::FRT	p0.1229_2Δ*mcbABCDEFG*::FRT, AmpR, TetR	This study
0.1229 Δ*mctAB*::*cat*	p0.1229_3$\Delta^{2850–5473}$::*cat*, AmpR, TetR, CamR	(15)
0.1229 ΔB17::FRT Δ*mctAB*::*cat*	p0.1229_2Δ*mcbABCDEFG*::FRT, p0.1229_3$\Delta^{2850–5473}$::*cat*, AmpR, TetR, CamR	This study
0.1229 Δ*fur*::*cat*	AmpR, TetR, CamR	This study
PA2	O157:H7, stx_{2a}	(81)
PA2 Δ*cirA*::*kan*	KanR	This study
PA2.1	CirA.Gln24ArgfsTer35	This study
PA2.2	*cirA*.-329_-244del	This study
PA2.3	CirA.Leu35GlyfsTer51	This study
EDL933	O157:H7, stx_{1a} stx_{2a}	(87)
EDL933 Δ*tonB*::*cat*	CamR	This study
Plasmid	*Characteristics*	*Reference*
pKD3	CamR	(71)
pKD4	KanR	(71)
pKD46	P_{araC}-λ recombinase, AmpR	(71)
pCP11B	FLP recombinase, KanR	(88)
pKD46-Kan	KanR	(15)
pBAD24	P_{araC}, AmpR	(89)
pKP315	pBAD24::P_{araC}-*tonB*, AmpR	(90)
pBR322	AmpR, TetR	(91)
pBR322::*cirA*	AmpR, TetR	This study
pBR322::mcc1229	pBR322::p0.1229_3$^{2745–7950}$, TetR	(15)
pBR322::mcc1229Δ*mctA*	pBR322::p0.1229_3$^{2745–7950}$Δ(3084-3792), TetR	This study
pBR322::mcc1229Δ*mctB*	pBR322::p0.1229_3$^{2745–7950}$Δ(3831-5423), TetR	This study
pBR322::mcc1229Δ*mctC*	pBR322::p0.1229_3$^{2745–7950}$Δ(5426-6319), TetR	This study
pBR322::*mctAB*	pBR322::p0.1229_3$^{2745–5425}$, TetR	This study
pBR322::*mctABC*	pBR322::p0.1229_3$^{2745–6343}$, TetR	This study
pBR322::*mctC*	pBR322::p0.1229_3$^{5426–6343}$, TetR	This study
pBR322::*mctCDE*	pBR322::p0.1229_3$^{5426-7047}$, TetR	This study
pBR322::*mctE*	pBR322::p0.1229_3$^{7047–6703}$, TetR	This study
pBR322::*mctD*	pBR322::p0.1229_3$^{6706–6320}$, TetR	This study
pBR322::*mctDE*	pBR322::p0.1229_3$^{7047–6320}$, TetR	This study
pRS551	promoterless *lacZ*, AmpR, KanR	(73)

pRS551::*mctA*'-*lacZ*	AmpR, KanR	This study
pRS551::*mctB*'-*lacZ*	AmpR, KanR	This study
pRS551::*mctC*'-*lacZ*	AmpR, KanR	This study
pRS551::*mctE*'-*lacZ*	AmpR, KanR	This study
Primer	*Sequence*	*T_a (˚C)*
mcb_VF	GGGGCTTAAAGGGGTAGTGT	49
mcb_VR	CCTAACAACGCCACGACTTT	
ΔmctAB_KF	acacatttcgtacagcctttacactcggtgaattagcggccctagatgcaGTGTAGGCTGGAGCTGCTTC	67
ΔmctAB_KR	ttaaacctcatgttttgtgatatctataatctgtgctttaggtatattatCATATGAATATCCTCCTTAG	
ΔmctAB_VF	GAAGATATCGCACGCCTCTC	54.5
ΔmctAB_VR	CGCCTGTTTGGCTATATGTG	
cirA_KF	gcagtatttactgaagtgaaagtccgcccggttcgccgggcatcttctcaGTGTAGGCTGGAGCTGCTTC	72
cirA_KR	ctatttcttgtgcatggcctgtgttagcggtcgatgacgatggcgaaacgCATATGAATATCCTCCTTAG	
cirA_VF	CCCGACGCTTATCGATCAGGG	56
cirA_VR	TGGTCCGGCTTTCTGGGATG	
cirA_fwd	ggccctttcgtcttcaagaaGTTTCTCCCTTCCTTGCTAAG	57
cirA_rev	taagctgtcaaacatgagaaTCAGAAGCGATAATCCAC	
pBR322_cirF	TTCTCATGTTTGACAGCTTATC	45
pBR322_cirR	TTCTTGAAGACGAAAGGG	
pBR322_cirVF	GGGCGACACGGAAATGTTG	53
pBR322_cirVR	GCGCTAGCAGCACGCC	
fur_KF	aaagccaacctgcaggttggcttttctcgttcaggctggcGTGTAGGCTGGAGCTGCTTC	72
fur_KR	tctaatgaagtgaaccgcttagtaacaggacagattccgcCATATGAATATCCTCCTTAG	
fur_VF	GCCGCACGTTTGAGGAATTT	52
fur_VR	TTTGCCAGGGACTTGTGGTT	
pBR322_insF	GCAAAAACAGGAAGGCAAAATG	46
pBR322_insR	CTGTCAGACCAAGTTTACTC	
pBR322_mctAF	gtatatatgagtaaacttggtctgacagGAACCTACAACACATGTGTAAAACGTCAATG	60
pBR322_mctBR	tgccttcctgtttttgcTTTTAAACCTCATGTTTTGTG	57
pBR322_ mctCR	tgccttcctgtttttgcGGGGAAGCCCCCTTAGATTAATG	60
pBR322_mctDER	tgccttcctgtttttgcATATGCTTGCTTGGGAAATTC	60
pBR322_mctCF	taaacttggtctgacagATGAATAATCTTATAAAAAAGGAAATCATAGAAAAATTTAAGAAATATAATTTC	53
pBR322_mctEF	taaacttggtctgacagATATGCTTGCTTGGGAAATTC	58
pBR322_mctER	tgccttcctgtttttgcTCACACTACCTTCCTCATATC	
pBR322_mctDF	taaacttggtctgacagGTGACTAATTTTAAATCAGACTTAAATC	54
pBR322_mctDR	tgccttcctgtttttgcCCATTAATCTAAGGGGGC	

pBR322_insVF	TTTGCAAGCAGCAGATTACG	49
pBR322_insVR	GCCTCGTGATACGCCTATTT	
ΔmctA_F	CATAAAGCCCGTAATATAC	55
ΔmctA_R	AACACCCCCAATTATATATTTG	
ΔmctB_F	AAATGAATAATCTTATAAAAAAGGAAATC	57
ΔmctB_R	TTTATAATCCTTAAAGCCCG	
ΔmctC_F	CCATTAATCTAAGGGGGC	57
ΔmctC_R	TTTTAAACCTCATGTTTTGTG	
pRS551_mctAF	GAATTCTATAACCATTAAAAAACTTGATTACTATCTC	47
pRS551_mctAR	CCCGGGATCCTTAGAAGAACATCATC	
pRS551_mctBF	GAATTCCAAAAGAATCCATATCCAG	47
pRS551_mctBR	CCCGGGTAAGCAGGATCCTATTTCTCCTATTGAATC	
pRS551_mctCF	TAAGCAGAATTCGCTACACAGATTTAAG	49
pRS551_mctCR	TAAGCAGGATCCATAGTGCAATATATC	
pRS551_mctEF	TAAGCAGAATTCGCTGCATAGCTATGCATG	55
pRS551_mctER	TAAGCAGGATCCTATGACTGGGATTACTCT	
pRS551_VF	TGCCAGGAATTGGGGATC	51
pRS551_VR	GTTTTCCCAGTCACGACGTT	
qPCR_rrsH_F	CGATGCAACGCGAAGAACCT	60
qPCR_rrsH_R	CCGGACCGCTGGCAACAAA	
qPCR_mctA_3270F	AGCCTCAACATGCCTAACGG	60
qPCR_mctA_3420R	TGGATAATGGTGGAGGTAAGCAC	
qPCR_mctB_4389F	GCACTTAGCTCCAAATTCGC	60
qPCR_mctB_4567R	GCGGAGCTGATACCAAACAG	
qPCR_mctC_5589F	TGGCAAATGACAACTTTCCCG	60
qPCR_mctC_5715R	GCGCCATCACGTAAGCATTT	
qPCR_mctE_6547F	GATATGCGTCCAGCGAGGAT	60
qPCR_mctE_6450R	GCTTTCCCTGAAACACAAGCA	

758

Table 2. Colonization by PA2 in mice co-colonized by 0.1229 and derivatives.

Co-colonizing strain	*No. in group*	*No. colonized*	*Percent*
0.1229	36	6	17
0.1229 Δ*mctAB*::*cat*	11	0	0
0.1229 ΔB17::FRT	6	0	0
0.1229 ΔB17::FRT Δ*mctAB*::*cat*	12	0	0
None	28	28	100

759

Table 3. Clinical illness due to PA2 in mice co-colonized by 0.1229 or its derivatives.

Infection	*No. moribund or dead/total by 7 days PI*	*Percent*
PA2 alone	4/28	14%
0.1229 + PA2	14/36	39%

0.1229 Δ*mctAB*::*cat* + PA2	2/11	18%
0.1229 ΔB17::FRT + PA2	2/6	33%
0.1229 ΔB17::FRT Δ*mctAB*::*cat* + PA2	0/12	0%

760

761 **Acknowledgments**

762 This work was supported by grant 1 R21 AI130856-01A1 to E.G.D. by the National Institute of

763 Allergy and Infectious Diseases and by USDA National Institute of Food and Agriculture Federal

764 Appropriations to E.G.D. under project PEN04464 and accession number 1015714.

765

766 **Author Statements**

767 The authors declare that there are no conflicts of interest.